



Light history modulates growth and photosynthetic responses of a diatom to ocean acidification and UV radiation

Wei Li^{1,2} · Tifeng Wang¹ · Douglas A. Campbell⁴ · Kunshan Gao^{1,3}

Received: 6 January 2022 / Accepted: 8 June 2022
© The Author(s) 2022

Abstract

To examine the synergetic effects of ocean acidification (OA) and light intensity on the photosynthetic performance of marine diatoms, the marine centric diatom *Thalassiosira weissflogii* was cultured under ambient low CO₂ (LC, 390 μatm) and elevated high CO₂ (HC, 1000 μatm) levels under low-light (LL, 60 μmol m⁻² s⁻¹) or high-light (HL, 220 μmol m⁻² s⁻¹) conditions for over 20 generations. HL stimulated the growth rate by 128 and 99% but decreased cell size by 9 and 7% under LC and HC conditions, respectively. However, HC did not change the growth rate under LL but decreased it by 9% under HL. LL combined with HC decreased both maximum quantum yield (F_v/F_M) and effective quantum yield (Φ_{PSII}), measured under either low or high actinic light. When exposed to UV radiation (UVR), LL-grown cells were more prone to UVA exposure, with higher UVA and UVR inducing inhibition of Φ_{PSII} compared with HL-grown cells. Light use efficiency (α) and maximum relative electron transport rate ($rETR_{max}$) were inhibited more in the HC-grown cells when UVR (UVA and UVB) was present, particularly under LL. Our results indicate that the growth light history influences the cell growth and photosynthetic responses to OA and UVR.

Keywords Chlorophyll fluorescence · Growth · Light intensity · Ocean acidification · Pigmentations · UV radiation

Introduction

Increasing atmosphere CO₂ concentration due to human activities since the Industrial Revolution has occurred at a faster rate than in any previous geological period (Hönisch et al. 2012), increasing from a 280 μatm preindustrial level to the present level of ca. 415 μatm; it is expected to reach 1000 μatm within this century (A1FI scenario) (Gattuso

et al. 2015). Increasing concentrations of dissolved anthropogenic CO₂ in the ocean induces changes in the seawater carbonate system, with a decrease in pH, CO₃²⁻ and carbonate saturation state, and an increase of CO₂ and HCO₃⁻, leading to ocean acidification (OA) (Doney et al. 2009). In parallel, global warming has been suggested to enhance stratification and shoaling of the upper mixed layer, resulting in increased exposure to both visible and UV radiation (UVR) for the phytoplankton within this layer (Gao et al. 2020). As inorganic carbon sources (HCO₃⁻ and CO₂) and solar radiation are the principal factors controlling photosynthetic carbon fixation, these expected changes will have profound implications on marine primary production and the marine biological CO₂ pump.

Phytoplankton in the upper mixing layer often experiences different light intensities and daily dosages as the transmission of visible light and UVR varies spatially and temporally, with generally increasing transmission from coastal waters to the open ocean (Häder and Gao 2015). Moreover, due to differences in mixing rates under future model projected scenarios (Capotondi et al. 2012; Masson-Delmotte et al. 2021), the light intensities to which cells are exposed in the upper mixing layer would be more

Edited by Chengchao Chen.

✉ Kunshan Gao
ksgao@xmu.edu.cn

- ¹ State Key Laboratory of Marine Environmental Science & College of Ocean and Earth Science, Xiamen University, Xiamen 361005, China
- ² College of Life and Environmental Sciences, Huangshan University, Huangshan 245041, China
- ³ Co-innovation Center of Jiangsu Marine Bio-industry Technology, Jiangsu Ocean University, Lianyungang 222005, China
- ⁴ Biology Department, Mount Allison University, Sackville, NB E4L 1G7, Canada

diverse (Häder and Gao 2015). Cells living under low light levels may occasionally be exposed to UVR due to mixing. While low to moderate levels of UVR are known to sometimes stimulate photosynthetic carbon fixation of coastal phytoplankton (Gao et al. 2007), higher levels of PAR and/or UVR generally show adverse effects (Häder et al. 2015). Therefore, UVR can modulate phytoplankton responses to environmental changes (Jiang et al. 2021; Jin et al. 2017; Li et al. 2012).

A number of studies have documented the effects of OA on growth and physiological performances of marine phytoplankton groups or single species, but findings vary (Beardall et al. 2014) especially when other co-varying ecological drivers are combined (Gao et al. 2019b). The effects of OA on the growth of marine phytoplankton are influenced by PAR levels (Gao et al. 2012b; Li et al. 2014) and are altered by UVR (Boyd et al. 2018; Li et al. 2017; Litchman and Neale 2005). For example, the calcification processes of calcified algae under OA were found to be significantly inhibited by UVR (Gao et al. 2009; Gao and Zheng 2010). Negative effects of UVR on the photosynthetic performance (F_v/F_M) of PS II and relevant proteins (psbD removal rate, ratio of RbcL to psbA) of *Thalassiosira weissflogii* was exacerbated under high CO₂ and low pH (Gao et al. 2018). However, the evaluation of OA effects normally neglects interacting effects with other key environmental drivers, and how microalgal cells will acclimate and adapt to multiple stressors in future oceans needs to be explored (Boyd et al. 2018; Gao et al. 2019a, b).

Diatoms grown under different light histories may exhibit different responses to OA (Li et al. 2020) and UVR (Guan and Gao 2008). Here, we hypothesize that the low- and high-light growth histories for diatoms may regulate their responses to OA and UVR, and that photosynthetic performances of cells after long term acclimation to low light and lowered pH would be more sensitive to UV exposure.

Results

Growth, cell size and pigmentations

Based on a two-way ANOVA (all $P < 0.0001$) analysis, it was found that growth rates were significantly affected by light level and CO₂ both individually and interactively (Table 1). HL stimulated growth rate by 128% under LC and by 99% under HC (all $P < 0.0001$), with no significant change in growth between LC and HC under LL conditions ($P = 0.559$) (Fig. 1A). HC significantly decreased the growth rate by 9% in comparison with LC under HL ($P = 0.0019$) (Fig. 1A). The cell size was also significantly affected by light level ($P < 0.001$) but not by CO₂ ($P = 0.87$) (Table 1). HL decreased cell size by 9% ($P = 0.005$) under LC and by 7% ($P = 0.022$) under HC compared with growth under LL (Fig. 1B).

HL, both individually and interactively with CO₂, significantly affected the Chl *a*, Chl *c* and carotenoid concentrations (All $P < 0.05$) (Table 1). There was no significant difference in Chl *a*, Chl *c* and carotenoid between the CO₂

Table 1 Two or three-way ANOVA analysis of individual and interactive effects of culture light (L) and CO₂ (C) level and subsequent responses to UVR exposure on the measured parameters of *T. weissflogii*

Parameters	L		C		UVR		L*C		L*UVR		C*UVR		L*C*UVR	
	F	P	F	P	F	P	F	P	F	P	F	P	F	P
Growth	9.79	< 0.0001	9.79	0.01	–	–	25.41	< 0.01	–	–	–	–	–	–
Cell size	38.78	< 0.001	0.03	0.87	–	–	0.71	0.42	–	–	–	–	–	–
Chl <i>a</i>	29.28	< 0.001	1.29	0.29	–	–	7.26	0.03	–	–	–	–	–	–
Chl <i>c</i>	1060.00	< 0.0001	6.77	0.03	–	–	7.99	0.02	–	–	–	–	–	–
Carotenoid	29.76	< 0.001	3.14	0.11	–	–	5.48	0.05	–	–	–	–	–	–
Car/Chl <i>a</i>	0.53	0.49	10.24	0.01	–	–	6.84	0.03	–	–	–	–	–	–
F_v/F_M	0.01	0.99	101.20	< 0.0001	–	–	9.53	< 0.01	–	–	–	–	–	–
$\Phi_{PSII-CL}$	70.37	< 0.0001	57.33	< 0.0001	–	–	6.77	0.01	–	–	–	–	–	–
NPQ	13.41	< 0.001	2.13	0.17	–	–	0.13	0.88	–	–	–	–	–	–
$\Phi_{PSII-SS}$	22.51	< 0.0001	0.77	0.39	34.29	< 0.0001	8.11	0.01	8.41	< 0.001	1.22	0.32	1.32	0.29
α	0.26	0.62	13.55	< 0.0001	16.73	< 0.0001	6.01	0.02	3.52	0.03	0.44	0.73	0.66	0.59
rETR _{max}	486.05	< 0.0001	2.01	0.17	44.78	< 0.0001	4.86	0.03	1.58	0.21	1.03	0.39	1.06	0.38
E_k	544.55	< 0.0001	7.11	0.01	45.35	< 0.0001	0.01	0.91	2.99	0.05	0.36	0.78	0.99	0.41
Inh Φ_{PSII}	16.40	< 0.001	5.76	0.03	4.70	0.02	5.11	0.03	3.24	0.06	0.36	0.70	0.39	0.68

Significant difference of treatments was based on the *F* value and subsequent calculated *P* value and indicated with bold font. “–” Not involved; Car/Chl *a*: carotenoid/Chl *a*; $\Phi_{PSII-CL}$: Φ_{PSII} -culture light; $\Phi_{PSII-SS}$: Φ_{PSII} -solar simulator; Inh Φ_{PSII} : UVR-induced inhibition of Φ_{PSII}

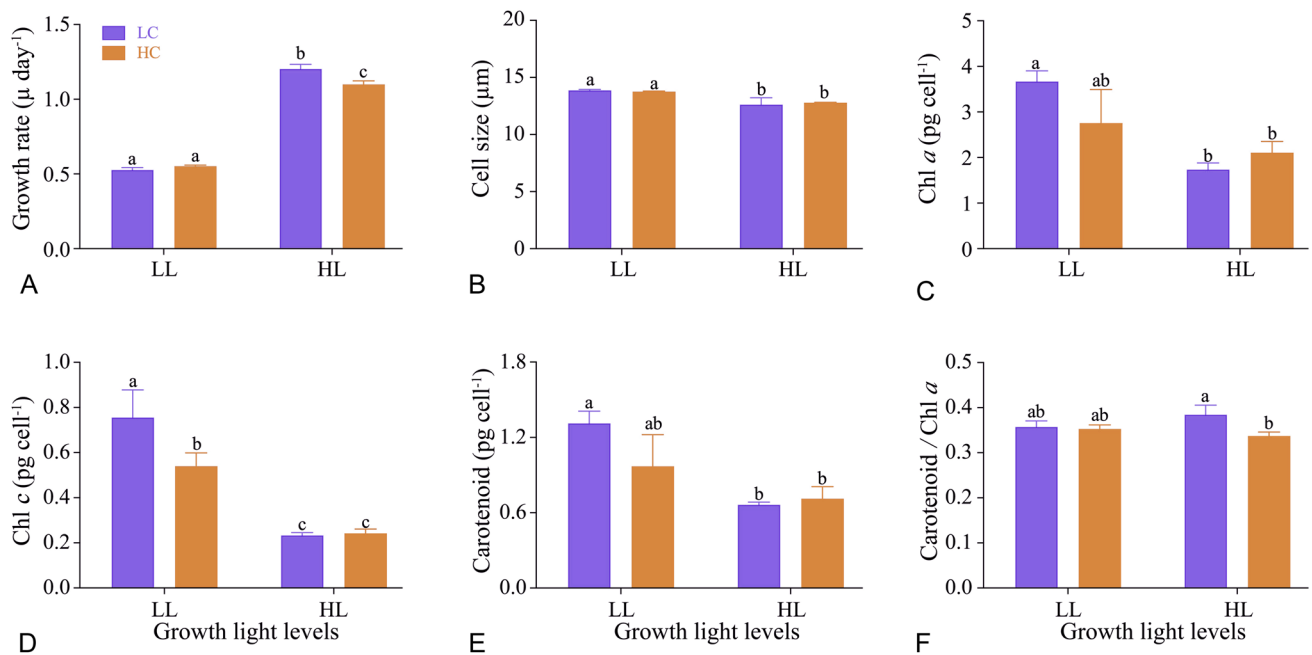


Fig. 1 Growth rate (A), cell size (B), Chl *a* (C), Chl *c* (D), carotenoid (E) and mass ratio of carotenoid to Chl *a* (F) of *T. weissflogii* grown under low light (60 μmol m⁻² s⁻¹, LL) and high light (220 μmol m⁻² s⁻¹, HL) levels, with low CO₂ (390 μatm, LC) and

high CO₂ (1000 μatm, HC) concentrations. Data are represented as means ± SD of triplicate cultures, and different letters above the bar indicate significant difference between treatments ($P < 0.05$)

treatments under either LL- or HL-grown cells (all $P > 0.05$) (Fig. 1C–E), except that Chl *c* decreased by 29% under HC compared to LC under LL ($P = 0.021$) (Fig. 1D). The ratio of carotenoid to Chl *a* did not change at LC compared to HC under LL conditions, however, under HL the ratio of carotenoid to Chl *a* significantly decreased by 12% under HC compared to LC ($P = 0.014$) (Fig. 1F).

Chlorophyll fluorescence

The trends of quantum yield (Φ_{PSII}) (Fig. 2A) and NPQ (Fig. 2B) derived from the fluorescence induction curves and the rapid light curve (Fig. 2C–F) of *T. weissflogii* grown under different light and CO₂ were shown in Fig. 2. There were no significant changes in F_v/F_M and Φ_{PSII} between LC and HC in HL-grown cells (all $P > 0.05$) (Fig. 3A, B); however, HC decreased F_v/F_M (Fig. 3A) and Φ_{PSII} (Fig. 3B) in LL-grown cells either measured under low (76 μmol m⁻² s⁻¹) or high (226 μmol m⁻² s⁻¹) actinic light ($P < 0.05$) derived from the induction curve (Fig. 2A). No significant change in NPQ was detected between LC and HC in any treatment ($P > 0.05$) (Fig. 3C). HL treatments did not alter the F_v/F_M , Φ_{PSII} or NPQ (Fig. 3A–C) at the same CO₂ level, except that a decrease of Φ_{PSII} under LC conditions was detected (Fig. 3B). Φ_{PSII} was significantly affected by culture light level and CO₂ individually and interactively based on a two-way ANOVA analysis (All $P < 0.05$).

No significant change in Φ_{PSII} was observed between LC and HC under either LL (Fig. 3D) or HL treatments ($P > 0.05$) (Fig. 3E), although exposure to UVR significantly decreased the Φ_{PSII} ($P < 0.05$) (Fig. 3D, E), except in the LC and LL treatment ($P > 0.05$) (Fig. 3D). By comparison, UVA induced higher inhibition of Φ_{PSII} in the LL-grown cells (both LC and HC) compared to UVB (Fig. 3F). The UVR (UVA + UVB)-induced inhibition of Φ_{PSII} on the LC and HC cultures were 14 and 30% in LL-grown cells, and 8% under both LC and HC in HL-grown cells (Fig. 3F).

Based on the characteristics of the rapid light curves (Fig. 2C–F; Table 2), significant inhibition of α in HC-grown cells occurred upon UV treatment (PA and PAB treatments) (three-way ANOVA, $P < 0.0001$), as reflected in the interactions of light with CO₂ (three-way ANOVA, $P = 0.02$) or UVR (three way ANOVA, $P = 0.03$). $r\text{ETR}_{\text{max}}$ of LL-grown cells were more sensitive to UVR treatments (PA and PAB treatments), especially under HC conditions. The culture light intensity, CO₂ concentration and UVR all showed significant effects on E_k (three-way ANOVA, all $P < 0.05$) (Table 1). Generally, the UVR-induced reduction of α , $r\text{ETR}_{\text{max}}$ and E_k was more pronounced in HC- and LL-grown cells when the cells were exposed to both UVA and UVB (Table 2).

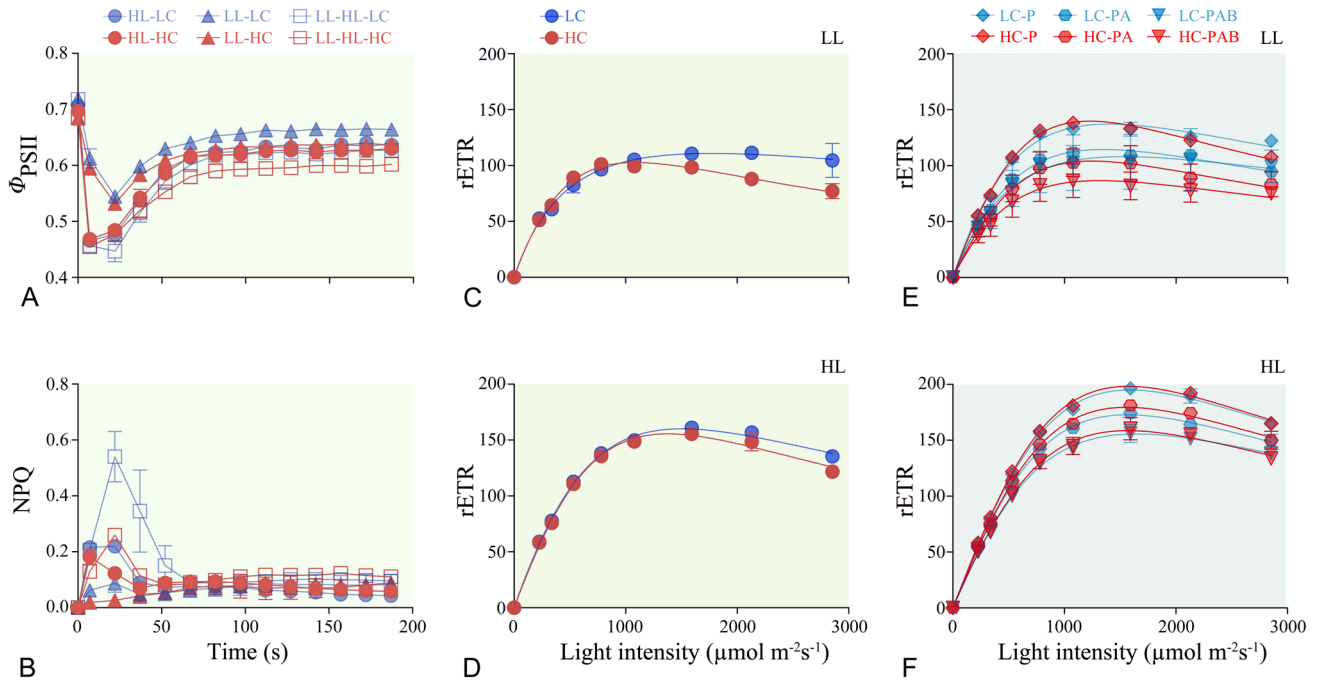


Fig. 2 The quantum yield (A) and NPQ (B) during the induction curve measurements and the rapid light curve (C–F) of *T. weissflogii* grown under low light ($60 \mu\text{mol m}^{-2} \text{s}^{-1}$, LL) (C, E) and high light ($226 \mu\text{mol m}^{-2} \text{s}^{-1}$, HL) (D, F) with low CO_2 (390 μatm , LC) and high CO_2 (1000 μatm , HC) treatments. Induction curve of high-light-grown cells measured with actinic light of $226 \mu\text{mol m}^{-2} \text{s}^{-1}$ (indicate as HL); low-light-grown cells measured with actinic

light of $76 \mu\text{mol m}^{-2} \text{s}^{-1}$ (indicate as LL) and $226 \mu\text{mol m}^{-2} \text{s}^{-1}$ (indicate as LL-HL). The rapid light curve of LL- (C, E) and HL-grown (D, F) cells were measured from its culture status (C, D) and after 1 h solar simulator exposure with PAR (P), PAR+UVA (PA) and PAR+UVA+UVB (PAB) (E, F). Data are represented as means \pm SD of triplicate cultures

Discussion

Our results show that predicted elevated pCO_2 , with resultant OA, decreased diatom growth rates and the cellular ratio of photoprotection to photosynthetic antenna pigment (carotenoid/Chl *a*) under the growth-saturating light levels (HL). This, however, caused as insignificant change in the growth rate under the growth rate-limiting light levels (LL). OA enhanced the sensitivity of the photosynthetic performance to UVA with exacerbated inhibition of Φ_{PSII} , rETR_{max} , α and E_k under LL.

The effects of OA on marine phytoplankton (diatom, coccolithophores, cyanobacteria etc.) have been well documented [see the reviews by Gao et al. (2019b) and Figuerola et al. (2021) and literature therein]. However, the effects differ due to species-specific energetics and physiological regulations under increased pCO_2 and decreased pH (Gao et al. 2012a). Elevated pCO_2 downregulates the energy consuming processes of CO_2 concentrating mechanisms (CCMs) (Reinfelder 2011), and may favor algal growth; however, the outcome of energy savings depends on the cellular energetic balance over energetic cost against acidic stress, resulting in positive, balanced or negative responses to OA (Gao et al. 2012b). Based on the documented results on the effects of

OA on the diatom *Thalassiosira weissflogii*, it appears that different strains, culture conditions (such as the CO_2 concentration/pH value, light intensity and light quality, photoperiod, temperature, nutrients levels and culturing methods) or acclimation time span (generations) are likely to be responsible for the observed differential responses (Supplementary Table S1). These documented results, together with the present work, further suggest that the effects of OA on diatoms be the result of multifactorial regulations and assessment of OA effects should take in situ environmental conditions into consideration. In this study, OA operated synergistically with HL to decrease the growth rate of *T. weissflogii*, indicating that the energy saved from CCM downregulation under HC conditions might exacerbate photorespiration at high light levels, so that HL–HC-grown cells lost more carbon to cope with the acidic stress, as shown previously in diatoms (Gao et al. 2012b; Qu et al. 2021).

Different light treatments can modulate morphological features and cellular pigmentations of phytoplankton (Finkel et al. 2010; Li et al. 2020). Changes of cell size may have significant implications on both light (Finkel 2001), nutrients and CO_2 absorption/diffusion (Armstrong 2008; Flynn et al. 2012) and subsequently influence the metabolic rate and community structure (Finkel et al. 2010; Marañón

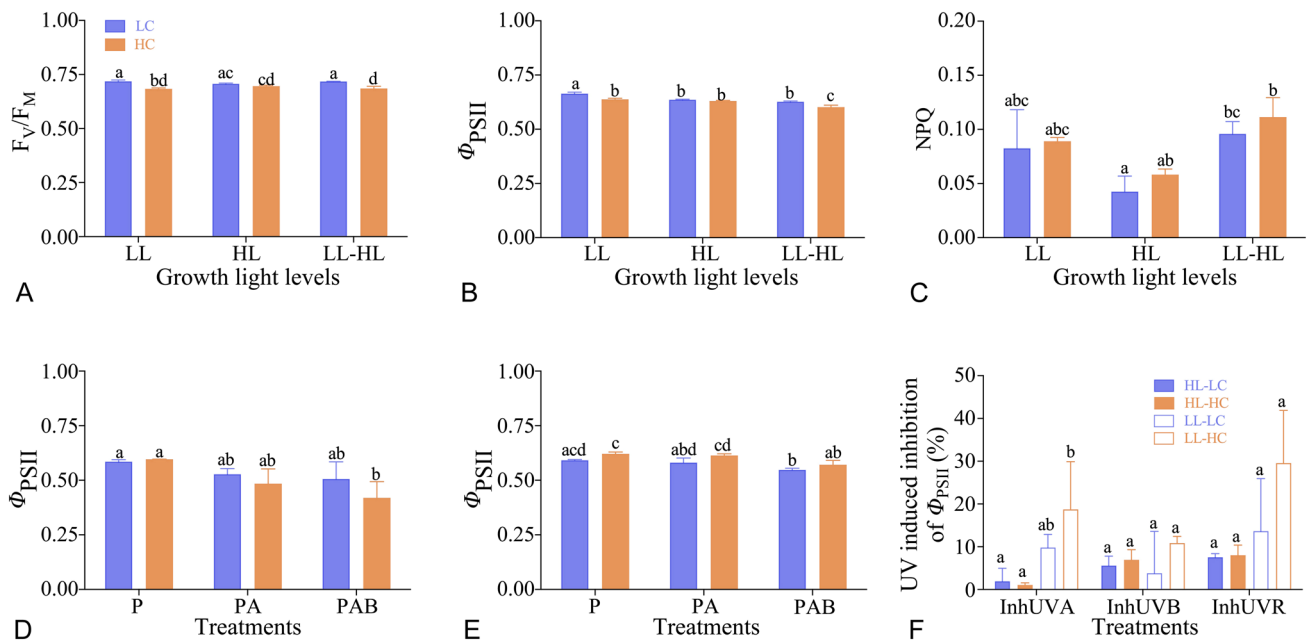


Fig. 3 The F_v/F_m (A), Φ_{PSII} (B) and NPQ (C) from last point of the induction curve in Fig. 2, and the measured Φ_{PSII} values after exposures under solar simulator to PAR (P), PAR+UVA (PA) and PAR+UVA+UVB (PAB) for 1 h of *T. weissflogii* grown under low light ($60 \mu\text{mol m}^{-2} \text{s}^{-1}$, LL) (D) and high light ($220 \mu\text{mol m}^{-2} \text{s}^{-1}$, HL) levels (E), with low CO_2 (390 μatm , LC) and high CO_2 (1000

μatm , HC) concentrations. UVA-, UVB- and UVR-induced inhibition of Φ_{PSII} are shown in F. Data are represented as means \pm SD of triplicate cultures, and different letters above the bar indicate significant difference between treatments ($P < 0.05$). LL-HL represents the cells grown under LL and measured at HL

Table 2 The fitted parameters of light using efficiency (α), maximum of relative electron transport rate ($r\text{ETR}_{\text{max}}$) and saturation light intensity (E_k) from rapid light curve of Fig. 2

	LL			HL		
	α	$r\text{ETR}_{\text{max}}$	E_k	α	$r\text{ETR}_{\text{max}}$	E_k
LC						
Initial	0.31 ± 0.06^a	112.4 ± 6.0^a	365.5 ± 47.3^a	0.28 ± 0.02^a	159.3 ± 3.4^a	577.8 ± 40.0^a
P	0.30 ± 0.01^a	135.8 ± 4.6^a	452.0 ± 35.7^{ab}	0.25 ± 0.01^{ab}	196.1 ± 4.8^b	789.1 ± 47.8^b
PA	0.24 ± 0.01^a	114.5 ± 6.6^a	479.7 ± 2.4^b	0.25 ± 0.01^b	173.0 ± 1.4^c	682.2 ± 27.5^{bc}
PAB	0.27 ± 0.03^a	115.8 ± 25.9^a	423.8 ± 47.6^{ab}	0.23 ± 0.01^b	158.0 ± 5.0^a	682.1 ± 49.3^{ac}
HC						
Initial	0.28 ± 0.02^a	102.2 ± 1.5^a	370.4 ± 26.2^a	0.26 ± 0.01^a	158.3 ± 4.8^a	600.0 ± 25.1^a
P	0.27 ± 0.00^a	138.6 ± 2.8^b	518.3 ± 13.6^b	0.26 ± 0.00^a	200.2 ± 3.6^b	780.9 ± 10.4^b
PA	0.19 ± 0.03^b	96.6 ± 14.4^a	518.1 ± 45.9^b	0.24 ± 0.00^{ab}	181.4 ± 3.3^c	742.6 ± 20.6^{bc}
PAB	0.19 ± 0.02^b	79.1 ± 14.3^a	427.4 ± 40.2^{ab}	0.22 ± 0.01^b	160.4 ± 7.7^a	715.8 ± 35.6^c

Data are presented as means \pm SD based on 3 biological replicates. Different letters indicate significant difference among light treatments (initial: culture light, P: PAR, PA: PAR+UVA, PAB: PAR+UVA+UVB) at a confidence level of 95% ($P < 0.05$)

2015). A decrease in light-harvesting pigments (both Chl *a* and some carotenoids), with a nearly balanced ratio of carotenoid to Chl *a* in HL-grown cells, reflects a photoacclimation strategy (Brunet et al. 2011; Janssen et al. 2001; Li et al. 2014, 2020) that prevents over-excitation of PSII electron transport (Gordillo et al. 2003; Xu and Gao 2012). In this study, a decrease in cell size along with decreased pigmentation under HL could have limited light absorption

and energy transfer, as pigment-specific light absorption increases as the cell size decreases (Fujiki and Taguchi 2002), giving higher light use efficiency (Jeffrey et al. 1996). Therefore, photophysiological down-regulation together with raised photorespiration and mitochondrial respiration (Gao et al. 2012b; Qu et al. 2021) could be responsible for the observed decrease in the growth rate of HL–HC-grown cells compared to LL–HC-grown ones (Fig. 1A).

The chlorophyll *a* fluorescence of PSII (F_V/F_M) is widely used as a stress indicator in algal physiology study (Beardall et al. 2001; Garcia-Gomez et al. 2014). In the HC treatment, the maximum (F_V/F_M) and effective quantum yield (Φ_{PSII}) of PSII were lowered under LL but not under HL, indicating that a restricted photon supply, coinciding with changes in pigment composition, must have affected the function of PSII. Although HL apparently compensated for the decrease in F_V/F_M and Φ_{PSII} in the HC-grown cells, it was not sufficient to balance the metabolic costs against the acidic stress associated with OA. Therefore, lowered or enhanced efficiency of energy transfer from photochemistry cannot reflect net biomass build-up or cell growth (Rokitta and Rost 2012).

High levels of UVR significantly affect morphological, photophysiological and biogeochemical properties of marine phytoplankton (Häder et al. 2007, 2015). The known effects differ depending upon other covaried environmental drivers. The light history to which cells have been acclimated influences their sensitivity to UVR exposures (Guan and Gao 2008). Compared to cells from shallow or surface layers, harmful effects of UVR on phytoplankton from deeper layers are generally more pronounced (Callieri et al. 2001; Neale et al. 1998). A higher ratio of damage rate to repair rate of PS II and therefore to drops in the abundance of key proteins (for example the psbA protein) and DNA repair upon UVR exposure of LL acclimated cells, may be possible reasons (Crawford et al. 2011). Since light saturation

intensity of LL-grown cells is lower compared to HL-grown ones, the LL-grown cells were more sensitive to high levels of PAR and UVR. This may be further exacerbated under HC condition as the acidic stress might exacerbate photoinhibition (Wu et al. 2010). OA treatment can exacerbate the stress of UVR on a marine diatom (Gao et al. 2018) and a coccolithophore (Gao et al. 2009). Nevertheless, OA could also eliminate UVR-induced inhibition of photochemical performances, as observed in a green microalga (Garcia-Gomez et al. 2014) and a diatom (Li et al. 2012). Previously, it has been shown that lowered environmental pH together with UVR exposures synergistically enhances synthesis of periplasmic proteins and carbonic anhydrase (Wu and Gao 2009). At lowered pH levels with elevated concentrations of H^+ in the environment, more protons are transported into the cells (Suffrian et al. 2011); however, the increased levels of carbonic anhydrase and periplasmic proteins can counter this by removing the extra protons to maintain intracellular homeostasis. Subsequently, the acidic stress was lessened and the photochemical performance improved. Here, LL-HC-grown cells were more prone to UVA alone and UVA + UVB-induced inhibition of Φ_{PSII} , α , $rETR_{max}$ and E_k . This signifies that the light history of cells can influence the impacts of OA and UVR on algal photosynthesis (Fig. 4).

Planktonic diatoms living in natural environments experience diverse light environments, varying across days and seasons and modulated by weather conditions and mixing

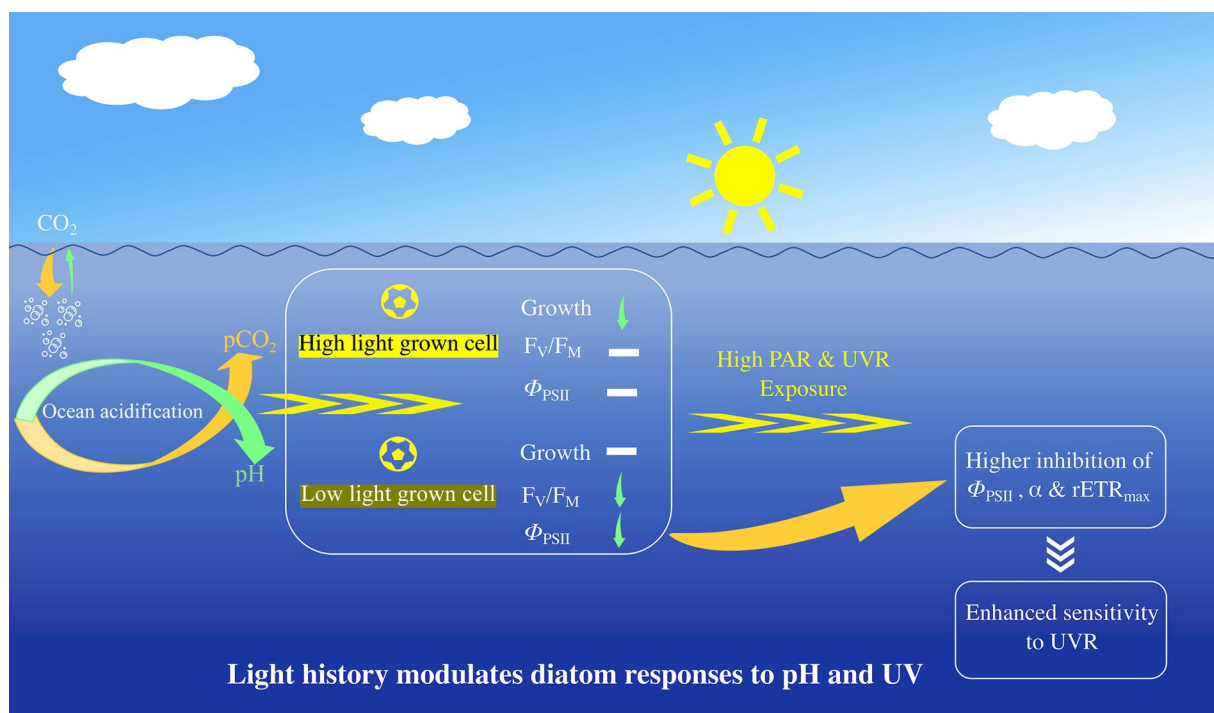


Fig. 4 A conceptual diagram illustrating that light history modulates growth and photosynthetic responses of diatom *T. weissflogii* to ocean acidification and UVR

rates in the water column. Since the light history to which diatom cells are acclimated has a significant influence on photosynthetic performance and growth under the influences of OA and UVR, as demonstrated in this work, diatom distributed in different areas and/or depths across different seasons may respond differently to OA and UVR. It should be pointed out that the short-term exposure to UVR in this work does not adequately reflect the performance of diatoms acclimated to solar radiation in the presence of UVR. However, such short exposure to UVR can be considered as a photobiological shock when microalgae from deeper layers are mixed up to surface layer due to perturbations, for example by typhoon-driven mixing. In conclusion, our results highlight the importance of considering the light history of diatoms when assessing their responses to OA and UVR.

Materials and methods

Algal culture

The diatom *Thalassiosira weissflogii* (CCMP1336) was acquired from the Center for Collections of Marine Algae (Xiamen University) and grown under cool white-fluorescent lamps at growth limited and saturated light levels ($60 \mu\text{mol m}^{-2} \text{s}^{-1}$, low light, LL; $220 \mu\text{mol m}^{-2} \text{s}^{-1}$, high light, HL) under low (390 μatm , low CO_2 , LC, ambient CO_2 concentration during March to May of 2013) or high CO_2 (1000 μatm , high CO_2 , HC) conditions. The LL treatments were achieved by covering the culture bottles (polycarbonate, Nalgene, Thermo Scientific) with a neutral density screen. Cells were semi-continuously cultured in bottles at 20 °C with a light:dark cycle of 12:12 (L:D) using artificial seawater enriched with Aquil medium (Morel et al. 1979). The cells in the above treatments were frequently diluted with freshly made medium that were pre-enriched with both LC and HC air using the CO_2 chamber (HP1000G-D, Ruihua, China). The dilution was carried out every 4 to 5 days, with cell concentration ranging from ca. 50 to 5000 cells ml^{-1} , which kept the pH (LL: 8.19 ± 0.01 and 7.87 ± 0.01 in LC and HC; HL: 8.21 ± 0.01 and 7.90 ± 0.02 in LC and HC) and carbonate system stable. Details for controlling the pH and carbonate system in the cultures were summarized in Gao (2021). Cells were grown under different light and CO_2 condition for ca. 20 generations before being used for subsequent measurements.

Growth rate and cell size determination

Cell number and cell size were measured with a Z2 Coulter Counter (Beckman, Buckinghamshire, UK). Growth rates (μ) were calculated according to the cell density change during a dilution cycle using the equation:

$$\mu = \frac{\ln N_A - \ln N_B}{T_A - T_B},$$

where N_A and N_B were cell number at time of T_A and T_B , respectively.

Pigmentation determinations

Cells grown for ca. 20 generations under the above CO_2 and light conditions were sampled onto GF/F filter (Whatman, 0.7 μm) and extracted using methanol (100%) (5 ml) at 4 °C for 12 h. After extraction, the supernatant was acquired by centrifuging the extract at 5000 g for 10 min (Universal 320R, Hettich, Germany) and then scanned with a spectrophotometer (DU800, Beckman, California, USA) to obtain optical densities at 470, 632, 653, 665, 666 and 750 nm. The Chl *a* and carotenoid were determined following Ryckebosch et al. (2011) which was modified from Wellburn (1994), and Chl *c* was determined following Ritchie (2006).

Chlorophyll fluorescence measurements

Chlorophyll fluorescence metrics from time induction curves under a fixed light or from rapid light curves were measured for *T. weissflogii* cells using a Xe-PAM (Walz, Germany). For the measurements of fluorescence induction curves, the saturation light pulse was set at 5000 $\mu\text{mol m}^{-2} \text{s}^{-1}$ for 0.8 s, and the LL-grown cells were measured at actinic light of 76 and 226 $\mu\text{mol m}^{-2} \text{s}^{-1}$, and for the HL-grown cells it was measured at actinic light of 226 $\mu\text{mol m}^{-2} \text{s}^{-1}$. The rapid light curves (RPLs) were measured at actinic lights of 0, 226, 337, 533, 781, 1077, 1593, 2130 and 2854 $\mu\text{mol m}^{-2} \text{s}^{-1}$ and then treated with a saturation light pulse of 5000 $\mu\text{mol m}^{-2} \text{s}^{-1}$ for 0.8 s after a 10 s exposure under each actinic light level. The F_v/F_M , Φ_{PSII} and NPQ under different culture conditions were obtained from the induction curves, and the calculation of parameters followed published equations (Bilger and Björkman 1990; Genty et al. 1989; Kitajima and Butler 1975). The maximum relative electron transport rate (rETR_{max}), light use efficiency (α) and saturation light intensity (E_k) were determined from RLC fit following Webb et al. (1974).

Solar UVR exposures

To investigate the photosynthetic responses to short-term UVR of *T. weissflogii* grown under different CO_2 and light conditions, the cells were transferred into 80 ml quartz tubes and exposed to a solar simulator for 1 h with 580 $\mu\text{mol m}^{-2} \text{s}^{-1}$ (ca. 134.5 W m^{-2}) of photosynthetically active radiation, 35 W m^{-2} of UVA and 2.5 W m^{-2} of UVB. The levels of PAR, UVA and UVB were chosen according to their daily average values of incident solar

radiation in the southern China during summer. Quartz tubes were wrapped with Ultraphan film 395 (UV Opak, DigeFra) to acquire PAR exposure (P) only; or with Folex 320 (Montagefolie, Folex, Dreieich, Germany) to filter the UVB range and to acquire PAR + UVA (PA) exposure; or with Ultraphan Film 295 (DigeFra, Munich, Germany) to acquire PAR + UVA + UVB exposure (PAB). The intensity of PAR, UVA and UVB were measured with a portable light meter (PMA-2100, Solarlight, USA). During the exposure under the solar simulator, tubes were placed in a temperature-controlled water bath at 20 °C (Eyela, CAP-3000, Tokyo Rikakikai Co. Ltd., Tokyo, Japan). Rapid Light Curves and Φ_{PSII} were measured after 1 h exposed to P, PA and PAB.

Statistics

Data were analyzed using SPSS 19.0 and Prism 9. Two- or three-way ANOVA were used to determine the individual and interactive effects of culture light intensity (low and high light), CO₂ concentrations (390 and 1000 μ atm) and UVR treatments (PAR, PAR + UVA, PAR + UVA + UVB) on the measured parameters, and Tukey's multiple comparison tests were used to determine differences between treatments at confidence level of 95% ($P < 0.05$).

Supplementary Information The online version contains supplementary material available at <https://doi.org/10.1007/s42995-022-00138-x>.

Acknowledgements This study was supported by the National Natural Science Foundation of China (41720104005, 41721005, 41890803), Key Research and Development Program of Anhui Province (202004i07020004), Excellent Youth Scholars Support Program of Anhui Province (gxyq2021212), MEL Visiting Fellowship Program (MELRS2008), and Research Platform of Eco-Environmental Protection Research Centre of Xin'an River Basin, Huangshan University (kypt202102). The authors are grateful to the laboratory engineers Xianglan Zeng and Wenyan Zhao for their logistical and technical support.

Author contributions KSG and WL designed the experiment. WL and TFW performed the research. WL and KSG analyzed the data. WL, KSG and DAC wrote the manuscript, and all authors revised the manuscript.

Data availability All data generated and analyzed during this study are included in this published article and its additional files.

Declarations

Conflict of interest The authors declare that they have no conflicts of interest. Author Kunshan Gao is one of the Editorial Board Members, but he was not involved in the journal's review of, or decision related to, this manuscript

Animal and human rights statement The authors declare that no animal and human are involved in this research.

Open Access This article is licensed under a Creative Commons Attribution 4.0 International License, which permits use, sharing, adaptation, distribution and reproduction in any medium or format, as long as you give appropriate credit to the original author(s) and the source, provide a link to the Creative Commons licence, and indicate if changes were made. The images or other third party material in this article are included in the article's Creative Commons licence, unless indicated otherwise in a credit line to the material. If material is not included in the article's Creative Commons licence and your intended use is not permitted by statutory regulation or exceeds the permitted use, you will need to obtain permission directly from the copyright holder. To view a copy of this licence, visit <http://creativecommons.org/licenses/by/4.0/>.

References

- Armstrong RA (2008) Nutrient uptake rate as a function of cell size and surface transporter density: a Michaelis-like approximation to the model of Pasciak and Gavis. *Deep Sea Res Pt I* 55:1311–1317
- Beardall J, Young E, Roberts S (2001) Approaches for determining phytoplankton nutrient limitation. *Aquat Sci* 63:44–69
- Beardall J, Stojkovic S, Gao K (2014) Interactive effects of nutrient supply and other environmental factors on the sensitivity of marine primary producers to ultraviolet radiation: implications for the impacts of global change. *Aquat Biol* 22:5–23
- Bilger W, Björkman O (1990) Role of the xanthophyll cycle in photo-protection elucidated by measurements of light-induced absorbance changes, fluorescence and photosynthesis in leaves of *Hedera canariensis*. *Photosynth Res* 25:173–185
- Boyd PW, Collins S, Dupont S, Fabricius K, Gattuso J-P, Havenhand J, Hutchins DA, Riebesell U, Rintoul MS, Vichi M (2018) Experimental strategies to assess the biological ramifications of multiple drivers of global ocean change—a review. *Glob Change Biol* 24:2239–2261
- Brunet C, Johnsen G, Lavaud J, Roy S (2011) Pigments and photoacclimation processes. In: Roy S, Llewellyn C, Egeland E, Johnsen G (eds) *Phytoplankton pigments: characterization, chemotaxonomy and applications in oceanography*. Cambridge University Press, Cambridge, pp 445–471
- Callieri C, Morabito G, Huot Y, Neale PJ, Litchman E (2001) Photosynthetic response of pico- and nanoplanktonic algae to UVB, UVA and PAR in a high mountain lake. *Aquat Sci* 63:286–293
- Capotondi A, Alexander MA, Bond NA, Curchitser EN, Scott JD (2012) Enhanced upper ocean stratification with climate change in the CMIP3 models. *J Geophys Res Oceans* 117:C04031
- Crawford KJ, Raven JA, Wheeler GL, Baxter EJ, Joint I (2011) The response of *Thalassiosira pseudonana* to long-term exposure to increased CO₂ and decreased pH. *PLoS ONE* 6:e26695
- Doney SC, Fabry VJ, Feely RA, Kleypas JA (2009) Ocean acidification: the other CO₂ problem. *Annu Rev Mar Sci* 1:169–192
- Figuerola B, Hancock AM, Bax N, Cummings VJ, Downey R, Griffiths HJ, Smith J, Stark JS (2021) A review and meta-analysis of potential impacts of ocean acidification on marine calcifiers from the Southern Ocean. *Front Mar Sci* 8:584445
- Finkel ZV (2001) Light absorption and size scaling of light-limited metabolism in marine diatoms. *Limnol Oceanogr* 46:86–94
- Finkel ZV, Beardall J, Flynn KJ, Quigg A, Rees TAV, Raven JA (2010) Phytoplankton in a changing world: cell size and elemental stoichiometry. *J Plankton Res* 32:119–137
- Flynn KJ, Blackford JC, Baird ME, Raven JA, Clark DR, Beardall J, Brownlee C, Fabian H, Wheeler GL (2012) Changes in pH at the exterior surface of plankton with ocean acidification. *Nat Clim Chang* 2:510–513

- Fujiki T, Taguchi S (2002) Variability in chlorophyll a specific absorption coefficient in marine phytoplankton as a function of cell size and irradiance. *J Plankton Res* 24:859–874
- Gao K (2021) Approaches and involved principles to control pH/pCO₂ stability in algal cultures. *J Appl Phycol* 33:3497–3505
- Gao K, Zheng Y (2010) Combined effects of ocean acidification and solar UV radiation on photosynthesis, growth, pigmentation and calcification of the coralline alga *Corallina sessilis* (Rhodophyta). *Glob Change Biol* 16:2388–2398
- Gao K, Wu Y, Li G, Wu H, Villafañe VE, Helbling EW (2007) Solar UV radiation drives CO₂ fixation in marine phytoplankton: a double-edged sword. *Plant Physiol* 144:54–59
- Gao K, Ruan Z, Villafañe VE, Gattuso JP, Helbling EW (2009) Ocean acidification exacerbates the effect of UV radiation on the calcifying phytoplankter *Emiliania huxleyi*. *Limnol Oceanogr* 54:1855–1862
- Gao K, Helbling EW, Häder D-P, Hutchins DA (2012a) Responses of marine primary producers to interactions between ocean acidification, solar radiation, and warming. *Mar Ecol Prog Ser* 470:167–189
- Gao K, Xu J, Gao G, Li Y, Hutchins DA, Huang B, Wang L, Zheng Y, Jin P, Cai X, Häder DP, Li W, Xu K, Liu N, Riebesell U (2012b) Rising CO₂ and increased light exposure synergistically reduce marine primary productivity. *Nat Clim Change* 2:519–523
- Gao G, Xu Z, Qi S, Wu H (2018) Increased CO₂ exacerbates the stress of ultraviolet radiation on photosystem II function in the diatom *Thalassiosira weissflogii*. *Environ Exp Bot* 156:96–105
- Gao G, Fu Q, Beardall J, Wu M, Xu J (2019a) Combination of ocean acidification and warming enhances the competitive advantage of *Skeletonema costatum* over a green tide alga, *Ulva linza*. *Harmful Algae* 85:101698
- Gao K, Beardall J, Häder D-P, Hall-Spencer JM, Hutchins DA (2019b) Effects of ocean acidification on marine photosynthetic organisms under the concurrent influences of warming, UV radiation, and deoxygenation. *Front Mar Sci* 6:322
- Gao K, Gao G, Wang Y, Dupont S (2020) Impacts of ocean acidification under multiple stressors on typical organisms and ecological processes. *Mar Life Sci Technol* 2:279–291
- Garcia-Gomez C, Gordillo FJ, Palma A, Lorenzo MR, Segovia M (2014) Elevated CO₂ alleviates high PAR and UV stress in the unicellular chlorophyte *Dunaliella tertiolecta*. *Photochem Photobiol Sci* 13:1347–1358
- Gattuso J-P, Magnan A, Billé R, Cheung W, Howes E, Joos F, Allemand D, Bopp L, Cooley S, Eakin CM, Hoegh-Guldberg O, Kelly R, Pörtner H-O, Rogers A, Baxter J, Laffoley D, Osborn D, Rankovic A, Rochette J, Turley C (2015) Contrasting futures for ocean and society from different anthropogenic CO₂ emissions scenarios. *Science* 349:aac4722
- Genty B, Briantais J-M, Baker NR (1989) The relationship between the quantum yield of photosynthetic electron transport and quenching of chlorophyll fluorescence. *Biochim Biophys Acta* 990:87–92
- Gordillo FJL, Figueroa FL, Niell FX (2003) Photon- and carbon-use efficiency in *Ulva rigida* at different CO₂ and N levels. *Planta* 218:315–322
- Guan W, Gao K (2008) Light histories influence the impacts of solar ultraviolet radiation on photosynthesis and growth in a marine diatom, *Skeletonema costatum*. *J Photochem Photobiol B Biol* 91:151–156
- Häder D-P, Gao K (2015) Interactions of anthropogenic stress factors on marine phytoplankton. *Front Environ Sci* 3:1–14
- Häder D-P, Kumar HD, Smith RC, Worrest RC (2007) Effects of solar UV radiation on aquatic ecosystems and interactions with climate change. *Photochem Photobiol Sci* 6:267–285
- Häder D-P, Williamson CE, Wängberg S-Å, Rautio M, Rose KC, Gao K, Helbling EW, Sinha RP, Worrest R (2015) Effects of UV radiation on aquatic ecosystems and interactions with other environmental factors. *Photochem Photobiol Sci* 14:108–126
- Hönisch B, Ridgwell A, Schmidt DN, Thomas E, Gibbs SJ, Sluijs A, Zeebe R, Kump L, Martindale RC, Greene SE, Kiessling W, Ries J, Zachos JC, Royer DL, Barker S, Marchitto TM, Moyer R, Pelejero C, Ziveri P, Foster GL et al (2012) The geological record of ocean acidification. *Science* 335:1058–1063
- Janssen M, Bathke L, Marquardt J, Krumbain WE, Rhiel E (2001) Changes in the photosynthetic apparatus of diatoms in response to low and high light intensities. *Int Microbiol* 4:27–33
- Jeffrey WH, Aas P, Lyons MM, Coffin RB, Pledger RJ, Mitchell DL (1996) Ambient solar radiation-induced photodamage in marine bacterioplankton. *Photochem Photobiol* 64:419–427
- Jiang X, Zhang Y, Hutchins DA, Gao K (2021) Nitrogen-limitation exacerbates the impact of ultraviolet radiation on the coccolithophore *Gephyrocapsa oceanica*. *J Photochem Photobiol B Biol* 226:112368
- Jin P, Ding J, Xing T, Riebesell U, Gao K (2017) High levels of solar radiation offset impacts of ocean acidification on calcifying and non-calcifying strains of *Emiliania huxleyi*. *Mar Ecol Prog Ser* 568:47–58
- Kitajima M, Butler WL (1975) Quenching of chlorophyll fluorescence and primary photochemistry in chloroplasts by dibromothymoquinone. *Biochim Biophys Acta* 376:105–115
- Li Y, Gao K, Villafañe V, Helbling E (2012) Ocean acidification mediates photosynthetic response to UV radiation and temperature increase in the diatom *Phaeodactylum tricoratum*. *Biogeosciences* 9:3931–3942
- Li Y, Xu J, Gao K (2014) Light-modulated responses of growth and photosynthetic performance to ocean acidification in the model diatom *Phaeodactylum tricoratum*. *PLoS ONE* 9:e96173
- Li W, Yang Y, Li Z, Xu J, Gao K (2017) Effects of seawater acidification on the growth rates of the diatom *Thalassiosira (Conticribra) weissflogii* under different nutrient, light, and UV radiation regimes. *J Appl Phycol* 29:133–142
- Li W, Wang T, Campbell DA, Gao K (2020) Ocean acidification interacts with variable light to decrease growth but increase particulate organic nitrogen production in a diatom. *Mar Environ Res* 160:104965
- Litchman E, Neale PJ (2005) UV effects on photosynthesis, growth and acclimation of an estuarine diatom and cryptomonad. *Mar Ecol Prog Ser* 300:53–62
- Marañón E (2015) Cell size as a key determinant of phytoplankton metabolism and community structure. *Annu Rev Mar Sci* 7:241–264
- Masson-Delmotte V, Zhai P, Pirani A, Connors SL, Péan C, Berger S, Caud N, Chen Y, Goldfarb L, Gomis MI, Huang M, Leit-zell K, Lonnoy E, Matthews JBR, Maycock JBR, Waterfield T, Yelekçi O, Yu R, Zhou B (2021) Climate change 2021: the physical science basis. Contribution of Working Group I to the Sixth Assessment Report of the Intergovernmental Panel on Climate Change
- Morel FMM, Rueter JG, Anderson DM, Guillard RRL (1979) Aquil: a chemically defined phytoplankton culture medium for trace metal studies. *J Phycol* 15:135–141
- Neale PJ, Davis RF, Cullen JJ (1998) Interactive effects of ozone depletion and vertical mixing on photosynthesis of Antarctic phytoplankton. *Nature* 392:585–589
- Qu L, Campbell DA, Gao K (2021) Ocean acidification interacts with growth light to suppress CO₂ acquisition efficiency and enhance mitochondrial respiration in a coastal diatom. *Mar Pollut Bull* 163:112008
- Reinfelder JR (2011) Carbon concentrating mechanisms in eukaryotic marine phytoplankton. *Annu Rev Mar Sci* 3:291–315

- Ritchie RJ (2006) Consistent sets of spectrophotometric chlorophyll equations for acetone, methanol and ethanol solvents. *Photosynth Res* 89:27–41
- Rokitta SD, Rost B (2012) Effects of CO₂ and their modulation by light in the life-cycle stages of the coccolithophore *Emiliana huxleyi*. *Limnol Oceanogr* 57:607–618
- Ryckebosch E, Muylaert K, Eeckhout M, Ruysen T, Foubert I (2011) Influence of drying and storage on lipid and carotenoid stability of the microalga *Phaeodactylum tricorutum*. *J Agric Food Chem* 59:11063–11069
- Suffrian K, Schulz KG, Gutowska MA, Riebesell U, Bleich M (2011) Cellular pH measurements in *Emiliana huxleyi* reveal pronounced membrane proton permeability. *New Phytol* 190:595–608
- Webb WL, Newton M, Starr D (1974) Carbon dioxide exchange of *Alnus rubra*. *Oecologia* 17:281–291
- Wellburn AR (1994) The spectral determination of chlorophylls a and b, as well as total carotenoids, using various solvents with spectrophotometers of different resolution. *Plant Physiol* 144:307–313
- Wu H, Gao K (2009) Ultraviolet radiation stimulated activity of extracellular carbonic anhydrase in the marine diatom *Skeletonema costatum*. *Funct Plant Biol* 36:137–143
- Wu Y, Gao K, Riebesell U (2010) CO₂-induced seawater acidification affects physiological performance of the marine diatom *Phaeodactylum tricorutum*. *Biogeosciences* 7:2915–2923
- Xu J, Gao K (2012) Future CO₂-induced ocean acidification mediates the physiological performance of a green tide alga. *Plant Physiol* 160:1762–1769